JCTC Journal of Chemical Theory and Computation

ARTICLE

pubs.acs.org/JCTC

Accurate Intermolecular Potentials with Physically Grounded Electrostatics

Maxim Tafipolsky* and Bernd Engels*

Institut für Physikalische und Theoretische Chemie, Universität Würzburg, Am Hubland, D-97074 Würzburg, Germany

ABSTRACT: A strategy is proposed to include the missing charge penetration energy term directly into a force field using a sum over pairwise electrostatic energies between spherical atoms as originally suggested by Spackman. This important contribution to the intermolecular potential can be further refined to reproduce the accurate electrostatic energy between monomers in a dimer by allowing for the radial contraction−expansion of atomic charge densities. The other components of a force field (exchange-repulsion and dispersion) are parametrized to reproduce the accurate data calculated by symmetry-adapted perturbation theory (SAPT). As a proof-of-concept, we have derived the force field parameters suitable for modeling intermolecular interactions between polycyclic aromatic hydrocarbons (PAH). It is shown that it is possible to have a balanced force field suitable for molecular simulations of large molecules avoiding error cancellation to a large extent.

1. INTRODUCTION

Constructing a reliable potential energy surface, which describes the energy of an assembly of molecules as a function of the atomic positions, is still a challenging problem. In particular, the intermolecular forces are primarily responsible for aggregation of molecules in the condensed phase.[1−3] Due to the size of the system, however, high-quality fully ab initio calculations are computationally very demanding, even more so when dynamics is to be studied (see, for example, refs 4 and 5). The force field methods are therefore indispensable for elucidating the properties of large aggregates of molecules. To be useful, parametrized force fields should be able to treat both intra- and intermolecular interactions accurately and reliably.

Large conjugated π systems, such as polycyclic aromatic hydrocarbons (PAH) and their derivatives (used as dyes), present notorious difficulties for modelers. A particular arrangement of monomers in an aggregate is ruled by a subtle interplay between electrostatic forces and dispersion interactions between extended aromatic π systems. Furthermore, the accurate structure and dynamics of this class of molecules within their crystalline environment are of primary importance for their optoelectronic properties (absorption, energy, and charge transport), needed for use in, for example, organic solar cells.[6] Due to the extensive π-conjugation with highly anisotropic charge distribution, the accurate description of intermolecular energies is extremely difficult, and literature force fields are too generic to be useful.

Quantum mechanical electronic structure calculations are helping to improve upon our understanding of the forces acting between molecules. The theory of intermolecular interactions[7,8] is now widely used to shed light on the particular forces responsible for aggregation of molecules in the condensed phase. Energy decomposition analysis (EDA) pioneered by Morokuma has been refined to such an extent (for a review, see ref 9) that it can be used as a reference for deriving all necessary contributions to the intermolecular interaction energy assuming additivity of the force field terms, such as electrostatic, exchange-repulsion, induction, and dispersion (see, for example, ref 10). On the other hand, intermolecular perturbation theory has emerged as a very powerful tool for the developing of model potentials.[11] Recent developments within the Symmetry Adapted Perturbation Theory (SAPT) enable highly accurate studies of intermolecular interactions at a level comparable to state-of-the-art methods such as coupled-cluster theory, CCSD(T), but with much reduced computational effort.[12−21] The efficient implementations[22,23,18] of this theory[24] allow for a deeper understanding of different contributions to the intermolecular interactions, thus giving a more detailed picture in comparison with the supermolecular approach, where only the total interaction energy is available as reference data. There exist several attempts in the literature to parametrize the intermolecular force fields on the basis of intermolecular perturbation theory (including SAPT) data.[25−28,12,29−33]

The reliability of a force field is based on its ability to reproduce some reference total intermolecular potential with good accuracy. In other words, it should describe the repulsion−attraction forces in a broad range of intermolecular distances and orientations in a balanced way. That this is not always the case for standard force fields can be illustrated with the help of the benzene dimer. With the highly accurate data calculated by SAPT for this dimer at hand, the interaction energy, being a sum of physically significant contributions, can be directly compared with the corresponding force field terms. This comparison indicates that standard force fields do not always capture the subtle balance between the two important contributions, namely, electrostatic and van der Waals terms (for some recent studies, see refs 16, 33−42). This is mainly due to the fact that the parameters of the majority of (empirical) force fields were optimized to reproduce the total interaction energy and/or thermodynamic data in the condensed phase. To make this point even more clear, we have calculated separate contributions to the total intermolecular potential for the benzene dimers using two

Received: March 17, 2011
Published: May 16, 2011

different orientations (sandwich and T-shaped), as depicted in Figure 1. The results are shown graphically in Figures 2 and 3.

We have chosen three different force fields where the electrostatic interactions are described by point charges (OPLS-AA[43]), bond dipoles (MM3[44,45]), or atomic multipoles up to quadrupoles (AMOEBA[46]), as implemented in the TINKER program package.[47] van der Waals interactions are represented in these force fields with three different functional forms as well: Lennard-Jones (OPLS-AA), modified Buckingham (MM3), and Buffered-14-7 (AMOEBA). We note that, in contrast to OPLS-AA and MM3, the AMOEBA force field is a polarizable one capable of including nonpairwise-additive many body effects in the force field via induced dipoles. The reference energies are taken from ab initio SAPT(DFT) calculations.[48] An examination of Figures 2 and 3 shows that for both configurations of the benzene dimer the electrostatic energy is substantially underestimated (below 4 and 5 Å for the sandwich and T-shape dimers, respectively), which is entirely due to a neglect of the charge penetration effects not accounted for by the force field. At the same time, van der Waals interactions are underestimated for the sandwich dimer in all three types of force fields (below 4 Å), whereas for the T-shaped dimer, the reference data, calculated as a sum of exchange−repulsion and dispersion contributions (see below), closely match the values from the OPLS-AA force field where the corresponding points (see Figure 3, center) almost coincide with their reference counterparts. If we look now at the total energy, it is evident that none of these force fields is able to describe both configurations equally well. As can be seen, OPLS-AA and MM3 are the best choices for treating sandwich and T-shaped dimers, respectively. They show poor results, however, for the other configuration, which is of course an unpleasant situation.

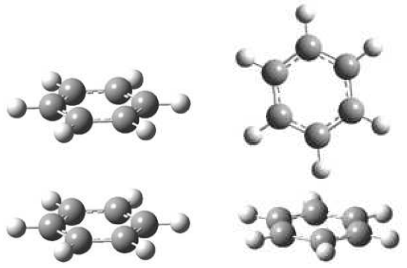

Figure 1. Sandwich (left) and T-shaped (right) configurations of the benzene dimer (carbon and hydrogen atoms are shown in black and white, respectively).

In this contribution, we seek a force field for PAHs which can treat all configurations equally well. Moreover, it is our objective to include more physics in the force field and not just simply reoptimize the parameters on the basis of the calculated overall intermolecular energy. Our preliminary tests using highly accurate total intermolecular interaction energies available in the literature for the benzene dimer[49] clearly indicate that it is not sufficient to reparameterize the van der Waals parameters utilizing simple functional forms used in current force fields, but incorporating the right physics of the electrostatic interactions is essential for simulations in the condensed phase (see below). To accomplish this task in a balanced way, both the electrostatic and van der Waals terms should be improved simultaneously. In contrast to some previous studies, our approach is based on the explicit inclusion of the short-range term due to charge penetration. In the present work, this term is treated separately from other short-range contributions (exchange-repulsion), as suggested recently by Spackman.[50] It also differs from other approaches, such as damping the long-range (multipolar) part of the electrostatic energy.[51,52] It mimics to some extent a more computationally expensive representation of electrostatic interactions with the Gaussian Multipole Model[53,54] and is similar in spirit to a recent work from Wang and Truhlar.[32] The importance

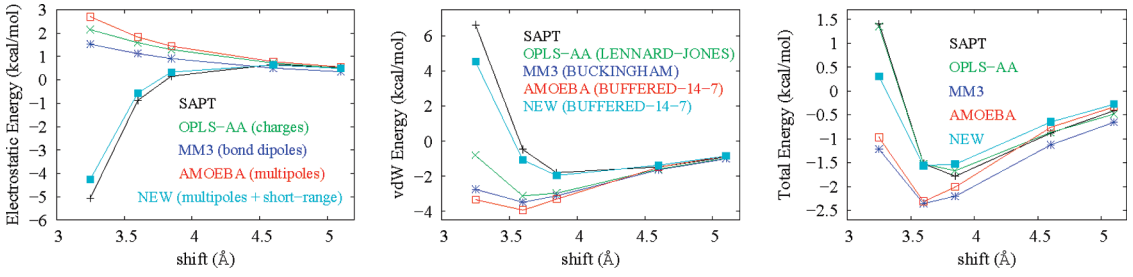

Figure 2. Electrostatic (left), van der Waals (center), and the total interaction energy (right) for the sandwich configuration of the benzene dimer (in kcal/mol). Shift is the distance (in Å) between the two benzene rings (see Figure 1). The reference data are taken from van der Avoird et al.[48] Lines are drawn to guide the eye.

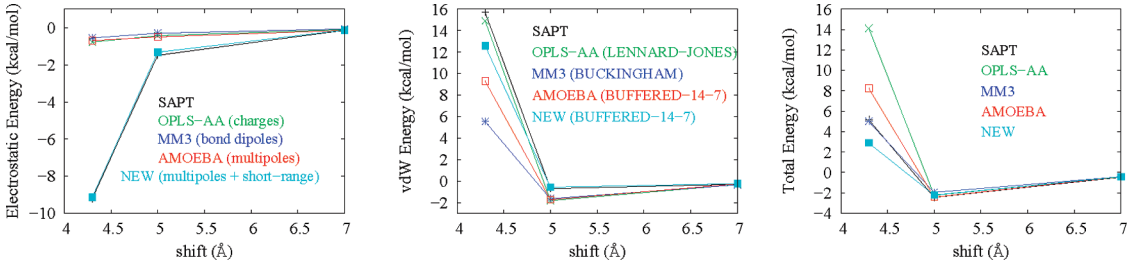

Figure 3. Electrostatic (left), van der Waals (center), and the total interaction energy (right) for the T-shaped configuration of the benzene dimer (in kcal/mol). Shift is the distance (in Å) between the center-of-mass of the two benzene rings (see Figure 1). The reference data are taken from van der Avoird et al.[48] Lines are drawn to guide the eye.

of charge penetration effects has been recognized in many previous studies, and various approaches have been proposed to include these effects with varying degrees of success (see, for example, refs 53, 55, and 56).

As a reference, we will use highly accurate results from SAPT calculated for a number of small aromatic dimers (benzene, naphthalene, anthracene) to develop the intermolecular force field suitable for molecular simulation of PAHs.

2. FORCE FIELD DEFINITION

In the present work, we use as a reference the results calculated with SAPT utilizing a density-functional theory (DFT) representation of the monomers taken from the work of van der Avoird et al.[48] (benzene), Podeszwa and Szalewicz[57] (naphthalene, anthracene, and pyrene), and Podeszwa (coronene).[58] Within the SAPT methodology, the total interaction energy is represented as a sum of several terms: electrostatic and exchange−repulsion (first-order), induction (polarization), exchange−induction, dispersion, and exchange−dispersion (second order) together with induction and exchange−induction terms of the third and higher orders. As a counterpart of van der Waals interactions in the force field, we use the sum of three terms calculated by SAPT: exchange−repulsion, dispersion, and exchange−dispersion terms, whereas the sum of induction and exchange−induction (second order) energies is used to represent the induction energy to be compared with the induction (polarization) energy from a polarizable force field.

It has been established that an anisotropic charge distribution is difficult (if not impossible) to describe with the widely used point charge models but should include higher multipoles as well (see, for example, refs 11, 59, 60). In this work, we represent the long-range part of the electrostatic energy with atom-centered multipoles up to quadrupoles as implemented in the TINKER program package (AMOEBA force field).[47] Atomic multipoles were calculated with the Distributed Multipole Analysis (GDMA) program[61,62] from wave functions calculated using the Gaussian program package.[63] The hybrid density functional, B3LYP,[64−66] together with the augmented correlation consistent basis sets, aug-cc-pVXZ (X = D, T),[67] was employed for all atoms if not stated otherwise. The monomers were kept rigid at the geometries used in the SAPT calculations (see above). If not available, the electrostatic interaction energies between monomers (perylene) were calculated with the SPDF program.[68] Since distributed multipoles in TINKER are restricted to quadrupoles, we use a locally modified version of the program written by Kisiel[69] to include all contributions up to hexadecapole−hexadecapole interactions for testing and validation purposes.

In this work, charge penetration is explicitly included in order to account for short-range quantum effects that are not accounted for by the classical multipolar expansion valid only at long range. Recently, Spackman[50] showed that it is possible to estimate this short-range contribution to the exact electrostatic energy by using a sum of classical Coulomb interaction between spherical atomic charge densities (so-called promolecular densities). In this case, the Coulombic energy between any two atoms separated by a distance R is calculated by the formula

$$E_{ab}(R) = \frac{Z_a Z_b}{R} - \int_{-\infty}^{\infty} \frac{Z_a \rho_b(r_2)}{|R_a - r_2|}\,\mathrm{d}r_2 - \int_{-\infty}^{\infty} \frac{Z_b \rho_a(r_1)}{|R_b - r_1|}\,\mathrm{d}r_1 + \int\int_{-\infty}^{\infty} \frac{\rho_a(r_1)\rho_b(r_2)}{|r_1 - r_2|}\,\mathrm{d}r_1\,\mathrm{d}r_2 \quad (1)$$

It can be readily shown[50] that for spherical charge distributions, $\rho(r)$, this expression can be reduced to a one-dimensional integration in reciprocal space (in atomic units):

$$E_{ab}(R) = \frac{2}{\pi}\int_0^{\infty} [Z_a - f_a(s)][Z_b - f_b(s)]\frac{\sin(sR)}{sR}\,\mathrm{d}s \quad (2)$$

where Z_a is the nuclear charge of atom a, $f_a(s)$ is the atomic scattering factor for atom a as a function of the scattering vector s ($= 4\pi \sin\theta/\lambda$) defined in terms of the spherical atomic electron density, $\rho(r)$, by the expression (e.g., for atom a)

$$f_a(s) = 4\pi\int_0^{\infty} \rho_a(r)\frac{\sin(sr)}{sr}\,\mathrm{d}r \quad (3)$$

The atomic scattering factors are obtained analytically from the atomic ground-state wave functions usually expanded with a linear combination of Slater-type functions. Several compilations of the atomic ground-state wave functions are available in the literature from Clementi and Roetti,[70] Bunge et al.,[71] and Su and Coppens.[72] In our work, we used closed-form expressions for the Fourier−Bessel transform of Slater-type functions developed by Su and Coppens.[73] For a recent implementation of Spackman's original ideas, see ref 74. As Spackman has noted, a contraction of the charge density of the hydrogen atom (Slater exponent) is needed to reproduce the reference electrostatic energies of a number of dimers with hydrogen bonds. The question now remains: how can one estimate the value of this contraction (or expansion)? It turns out that it can be done rather straightforwardly by rewriting the last equation in the following form:[75]

$$E_{ab}(R) = \frac{2}{\pi}\int_0^{\infty} [Z_a - f_a(s/\kappa_a)][Z_b - f_b(s/\kappa_b)]\frac{\sin(sR)}{sR}\,\mathrm{d}s \quad (4)$$

where the radial dependence of the spherical charge densities of atoms a and b is modified by expansion−contraction parameters ("kappa"), κ_a and κ_b, respectively. A similar approach has been used in the refinement of the spherical pseudoatom charge densities based on accurate X-ray diffraction data.[75] Therefore, we extend the approach of Spackman by allowing for the radial contraction ($\kappa > 1$) or expansion ($\kappa < 1$) for spherical atomic densities. The integral in eq 4 was evaluated numerically as suggested by Spackman[50] (see also refs 22 and 24 therein) using routines from ref 76.

For the pairwise additive van der Waals (vdW) interactions, we have adopted the buffered 14−7 functional form[77] used in the AMOEBA force field (for details, see ref 46). It is, however, necessary to adjust the vdW parameters appropriately,[50] since the electrostatic part of the force field is modified by adding the short-range interactions as described above. In this work, we reoptimize the vdW parameters (two for each atom class) using this particular function, but in principle, any functional form can be used instead.

Induction (polarization) is the interaction of an induced dipole on one fragment with the permanent dipole on another fragment, expressed in terms of the dipole polarizability. The efficacy of truncating the polarizability expansion at the first (dipole) term is due to the treatment of this term in a distributed manner. In the AMOEBA force field, the molecular polarizability is expressed as a sum over atomic isotropic dipole polarizabilities. Iterating the dipole-induced dipole interaction to self-consistency captures many body effects. We adopted the parameters (atomic isotropic polarizabilities and damping factor) from the AMOEBA force field,[46] i.e., 1.750 for carbon and 0.696 Å^3 for

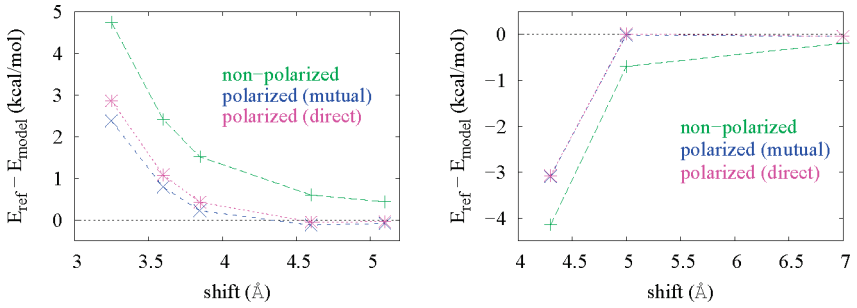

Figure 4. The difference in the total interaction energy for the sandwich (left) and T-shaped (right) configurations of the benzene dimer (in kcal/mol) with and without the polarization term included. Shift is the distance (in Å) between the two benzene rings (see Figure 1). The "direct" dipole polarization avoids an iterative calculation by using only the permanent electric field in computation of induced dipoles, whereas in the "mutual" polarization one iterates the induced dipoles to self-consistency. The reference data are taken from van der Avoird et al.[48] Dashed lines are drawn to guide the eye.

hydrogen in aromatic rings. There is an indication, however, that the aromatic carbon bridging two aromatic rings (i.e., all its neighbors are carbons) should have a somewhat larger polarizability.[78] In principle, all parameters for the dipole induction model used in AMOEBA can be reoptimized to reproduce the induction energy (quenched by the exchange-induction contribution) calculated by SAPT as well. Furthermore, the static molecular polarizability tensors calculated with the default parameters for a number of polycyclic aromatic molecules are in accord with the exact values (see below), confirming the results from ref 46. The influence of the polarization energy for the benzene dimers can be appreciated from Figure 4, where the total energies calculated with and without (switched off) the polarization term are compared with their reference counterparts.[48] In TINKER, two options for the incorporation of the polarization term in the force field are available so that one can select between the use of direct and mutual dipole polarization. In the former approach ("direct"), an iterative calculation is avoided by using only the permanent electric field in computation of induced dipoles, whereas in the latter ("mutual") one an iteration of the induced dipoles to self-consistency is performed.

Despite the limited number of dimer configurations used, Figure 4 clearly shows that for benzene dimers the noniterative approach to the dipole polarization ("direct") can be a good approximation of a more elaborate iterative one ("mutual"). It can be seen that at shorter intermonomer distances the deviation from the SAPT calculated total intermolecular energies (E_{ref}) can be quite large. We also note that the simulated (AMOEBA) total energy underestimates (overestimates) their reference counterparts for the sandwich (T-shaped) configuration, regardless of the polarization model used in the force field.

3. PARAMETRIZATION STRATEGY

To fit the various parameters, we have implemented the short-range contribution to the electrostatic energy as described by Spackman[50] within the TINKER program package.[47] The expansion-contraction parameters for all symmetrically nonequivalent atoms (eq 4) were optimized with the genetic algorithm PIKAIA,[79] used successfully by one of the present authors (M.T.) to parametrize the intramolecular force field for metal−organic frameworks (for details, see ref 80). As a fitness function, we use the root-mean-square deviation (rmsd = $((\Sigma_{i=1}^{N}(E_{ref}^{i} - E_{model}^{i})^2)/N)^{1/2}$, where N is the number of dimer configurations) between the exact electrostatic energies calculated by SAPT for the dimer configurations and the sum of the long-range part (distributed

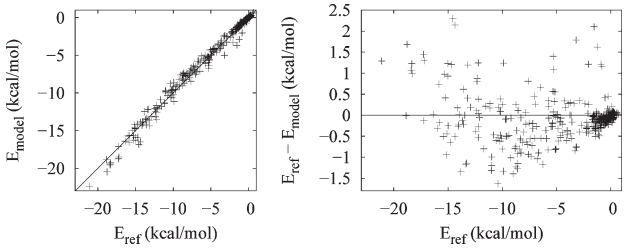

Figure 5. Scatter plots of electrostatic energies (left) and their differences (right) calculated for 500 benzene dimer configurations (in kcal/mol). The reference data are taken from van der Avoird et al.[48]

multipoles) and the short-range part represented by a sum of Coulombic interactions between spherical atoms. For comparison, the atomic scattering factors in eq 4 are calculated from the analytic atomic wave functions taken from three different sources mentioned above.[70−72] Since the results are very similar for all three compilations, only the results based on the data from Su and Coppens,[72] obtained using a nonlinear least-squares fitting of numerical relativistic atomic wave functions by a linear combination of Slater-type functions, will be discussed. The atomic multipoles are calculated from wave functions obtained at the B3LYP/aug-cc-pVDZ level of theory. This level of theory is found to be adequate for our purposes, confirming the results of Volkov et al.[81] However, to be consistent with the large basis set used in the SAPT calculations,[48,57] we employed here a larger aug-cc-pVTZ basis set for benzene, naphthalene, and anthracene as well. To get meaningful expansion−contraction parameters, the dimer configurations were selected with some care. For example, the T-shaped dimer configurations are found to be important for the refinement of the κ parameter for hydrogen in benzene and polycyclic aromatics.

For the vdW part of the force field, we reparametrize the values of the atom size (in Å) and homoatomic well depth (in kcal/mol), whereas a reduction factor for hydrogen atoms was kept unchanged. As a fitness function for the genetic algorithm, the RMSD between the SAPT data (as a sum of exchange−repulsion, dispersion, and exchange−dispersion terms) and the vdW part of the force field is used. In principle, the exchange-repulsion and dispersion (quenched by the exchange−dispersion term) contributions can be refined independently, but this would require a more substantial modification of the TINKER code.

The reference energies for naphthalene (35 configurations), anthracene (32 configurations), and pyrene (44 configurations)

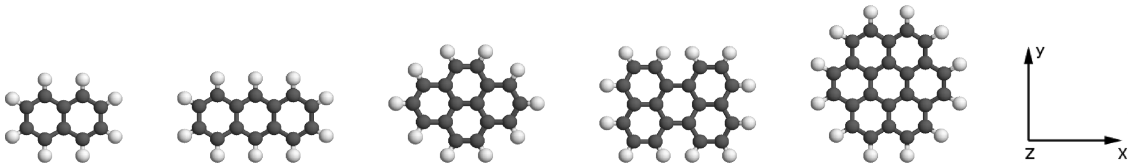

Figure 6. Molecular structure of selected PAHs (from left to right): naphthalene, anthracene, pyrene, perylene, and coronene (carbon and hydrogen atoms are shown in black and white, respectively).

Table 1. Expansion−Contraction (κ) Parameters for Carbon and Hydrogen in Several PAHs

	κ (C)	κ (H)	RMSD (kcal/mol)
	naphthalene (35 config.)		
Spackman	1.0	1.24	1.8
benzene	1.002	1.45	0.7
opt	1.012	1.42	0.3
	anthracene (32 config.)		
Spackman	1.0	1.24	3.1
benzene	1.002	1.45	1.5
opt	1.018	1.41	0.4
	pyrene (44 config.)		
Spackman	1.0	1.24	5.0
benzene	1.002	1.45	4.1
opt	1.024	1.4 (fixed)	0.6
	coronene (56 config.)		
Spackman	1.0	1.24	4.4
benzene	1.002	1.45	3.7
opt	1.022	1.4 (fixed)	1.4

dimers are taken from ref 57. The coronene dimer is probably the largest system calculated with SAPT (56 configurations).[58] In addition, highly accurate correlated calculations of the intermolecular potential surface in the coronene dimer have been published recently by Janowski et al.[4] For pyrene and coronene dimers, no T-shaped configurations were calculated using SAPT despite the recent finding that this arrangement for coronene might energetically compete with the stacked parallel orientations.[82,4]

The geometries of the monomers (see Figure 6) were optimized by Podeszwa et al.[57,58] using the B3LYP/6-31G(d) level of theory and were kept fixed in their dimer calculations.

4. RESULTS AND DISCUSSION

Electrostatic Energy. First, we turn to the benzene dimer. van der Avoird et al.[48] have calculated SAPT interaction energies and the corresponding physically meaningful contributions for a large number of dimer configurations (~500), which we use here as our reference. The scatter plot shown in Figure 5 compares the electrostatic energies calculated by the force field with the optimized expansion−contraction parameters for the carbon and hydrogen atoms (E_{model}) against the reference SAPT data (E_{ref}). During the refinement, all reference energy values are weighted equally (unit weights). The optimized κ value for the carbon atom (1.002) is very close to 1. The value of 1.45 obtained for the hydrogen atom is somewhat larger than that used by Spackman (1.24). The indicated contraction of the electron density of the hydrogen atom makes sense since, being attached to an aromatic carbon atom, it is positively charged. Interestingly, our value is very close to an average value (1.40) recommended by Coppens et al.[75] for the radial contraction of H in their spherical-atom X-ray refinements. The RMS deviation for the whole set of benzene dimers is only 0.47 kcal/mol. An examination of Figure 5 shows that the differences between the reference electrostatic energies and their force field counterparts are within 1 kcal/mol for the majority of dimer configurations. This validates the present approach used for the electrostatics. The mean difference ($= 1/N \sum_{i=1}^{N}[E^i_{ref} - E^i_{model}]$) of −0.07 kcal/mol signals that the simulated (force field) energies reproduce the reference data without a systematic error. It follows from Figures 2 and 3 that for the sandwich and T-shaped benzene dimer the new force field is in considerably closer agreement with the SAPT reference data as compared to the other force fields, reproducing the right physics of the electrostatic interactions especially at shorter intermolecular distances.

The κ values optimized for the benzene dimer are readily transferable to other PAHs. This is evident from the data presented in Table 1. It can be seen that the overall reproduction (measured by RMSD) of the electrostatic interaction energies for dimers of larger PAHs is quite satisfactory when the values optimized for the benzene dimer (labeled as "benzene") are used and that even small changes in the κ parameters (mainly for carbon) can improve the fit significantly (labeled as "opt"). We note that for larger PAHs one can refine the κ parameters for all symmetrically nonequivalent carbon atoms, which would definitely improve the fit even further, and we found that this is indeed the case. But to keep our model as simple as possible (with less parameters), we decided to optimize only one κ parameter for all aromatic carbons. The values used by Spackman are given for comparison. Figure 7 shows scatter plots of electrostatic energies for naphthalene, anthracene, pyrene, and coronene dimers calculated using the optimized κ parameters (labeled as "opt" in Table 1) against the SAPT reference data. Remarkably, with only two expansion−contraction parameters (for C and H), the agreement between the calculated electrostatic energies and their reference counterparts is fairly good over a wide range of energy values.

The significance of the short-range contributions to the electrostatic interaction energy even for relatively nonpolar PAHs can be appreciated from the data in Table 2 below. As an example, we took the perylene dimer (sandwich configuration) and calculated the accurate electrostatic energy by integration over the unperturbed charge densities of the monomers[68] (labeled as "true") as a function of the intermonomer distance (see Figure 8). The geometry of the perylene molecule was taken from the database of PAHs[83] (optimized at the B3LYP/6-31+G(d) level of theory). The point charges (labeled as "charges") were obtained by the fit to the electrostatic potential (ESP), as is usually routinely done. To this end, we use the Merz−Kollman sampling scheme[84] with ca. 2100 grid points

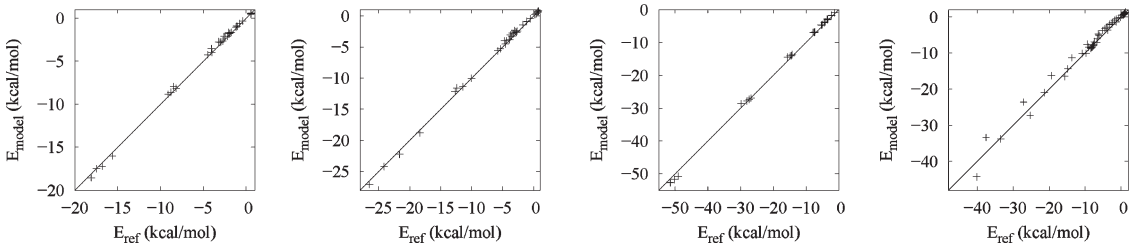

Figure 7. Scatter plots of electrostatic energies for selected dimers of PAHs (in kcal/mol). From left to right: naphthalene (35 configurations), anthracene (32 configurations), pyrene (44 configurations), and coronene (56 configurations). The reference data are taken from Podeszwa et al.[57,58]

Table 2. Short- and Long-Range Contributions to the Total Electrostatic Interaction Energy for the Perylene Dimer (in kcal/mol)[a]

		DMA[c]				
distance, Å	charges[b]	quadrupole	octupole	hexadecapole	kappa model[d]	"true"[e]
3.0	5.02	7.88	6.07	7.70	−49.84	−42.16
3.2	4.10	5.78	4.60	5.49	−26.93	−20.83
3.4	3.39	4.42	3.61	4.13	−14.57	−9.87
3.6	2.84	3.50	2.93	3.24	−7.69	−4.35
3.8	2.41	2.85	2.43	2.63	−4.02	−1.62
4.0	2.06	2.38	2.06	2.19	−2.17	−0.30
4.5	1.44	1.63	1.44	1.50	−0.42	0.66
5.0	1.06	1.19	1.07	1.10	0.03	0.72
5.5	0.80	0.90	0.82	0.84	−0.05	0.64
6.0	0.62	0.71	0.64	0.66	0.004	0.53

[a] B3LYP/aug-cc-pVDZ//B3LYP/6-31+G(d). The geometry of the monomer is taken from ref 83. [b] From ESP fit: Merz−Kollman sampling (~2100 points per atom); RMS = 0.71 kcal/mol. [c] Distributed multipole analysis using three different ranks of multipoles. [d] Sum over spherical atomic density Coulomb interactions using $\kappa(C) = 1.01$ and $\kappa(H) = 1.4$. [e] Numerical evaluation of the exact Coulomb integral over unperturbed charge densities of monomers.

per atom with a RMS deviation of 0.71 kcal/mol.[63] The long-range contribution to the electrostatic energy is then represented either with these point charges or with the atomically distributed multipoles[62] (labeled as "DMA") at three different levels (quadrupole, octupole, and hexadecapole). For example, at the hexadecapole level, all interactions up to hexadecapole−hexadecapole ones between all atoms belonging to the two different monomers are included. It should be also noted that the ESP calculated for the same set of grid points as used in the fit of point charges above is reproduced by distributed multipoles truncated at the quadrupolar level with a RMS deviation of 0.85 kcal/mol. Both the point charges from the fit and the atomic multipoles systematically overestimate (more negative on average) the reference ESP data (B3LYP/aug-cc-pVDZ//B3LYP/6-31+G(d)) with the mean difference of 0.2 kcal/mol.

A number of important conclusions can be drawn from these data. First, it can be clearly seen that at the intermonomer distances below 4 Å, both the point charge model and the atomic multipole model severely underestimate the electrostatic interaction in the dimer (compare with the last column of Table 2). We note that the average intermonomer distance in the crystal structure of the so-called α-form of perylene (the four perylene

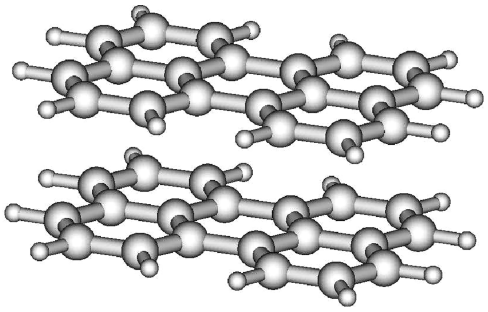

Figure 8. Sandwich configuration of the perylene dimer.

molecules in the unit cell are grouped in pairs about centers of symmetry) is found to be around 3.46 Å.[85] Thus, an approximation of the electrostatic energy either with point charges or with multipoles is inadequate. These models become valid above ca. 5 Å (see three last rows in Table 2). It can be seen that the charge penetration contribution to the electrostatic interaction for the perylene dimer is significant especially at intermonomer distances < 3.5 Å. This short-range contribution evaluated recently by Jenness et al.[86] for the water−acene series is much smaller in magnitude and is comparable with the long-range contribution due to atomic multipoles (up to quadrupoles on all carbon atoms). Second, we note that the multipole model truncated at the quadrupolar level would already do a good job in describing the long-range contribution to the electrostatic energy (in comparison with a much more computationally demanding hexadecapolar level). Finally, we see that the missing part (labeled as the "κ model"), calculated as the sum over spherical atomic density interactions using the optimized expansion−contraction (κ) parameters, is quite substantial. Combined with the multipole approximation for the long-range part (represented by the atomic multipoles up to and including quadrupoles), it recovers the total intermolecular electrostatic energy in the perylene dimers (10 sandwich configurations) with an RMS deviation of only 0.36 kcal/mol and a mean difference of −0.2 kcal/mol. Thus, with the optimized κ parameters at hand and assuming their transferability between chemically similar atoms, we can now estimate quite accurately the intermolecular electrostatic energy in the clusters of larger PAH molecules within seconds. For comparison, the numerical evaluation of the exact Coulomb integral for the perylene dimer (wave functions from B3LYP/aug-cc-pVDZ) using a serial version of the SPDF program[81] used here takes ca. 10 h on 1 CPU (Linux OS, x86_64 AMD, 2.933 GHz, 4 GB RAM).

Induction Energy. In principle, the quality of the polarization energy component of the AMOEBA force field[46] used here can

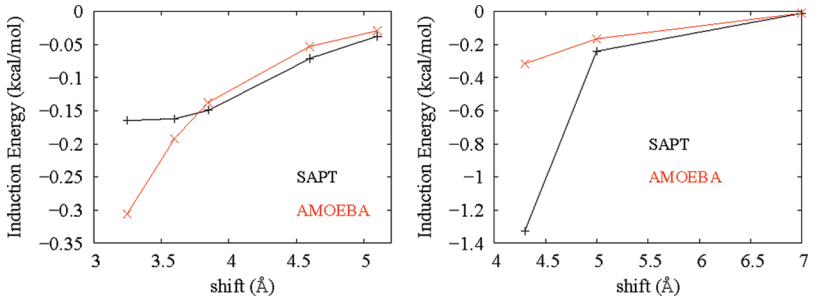

Figure 9. The induction energy for the sandwich (left) and T-shaped (right) configurations of the benzene dimer (in kcal/mol). Shift is the distance (in Å) between the two benzene rings (see Figure 1). The reference data are taken from ref 48. Lines are drawn to guide the eye.

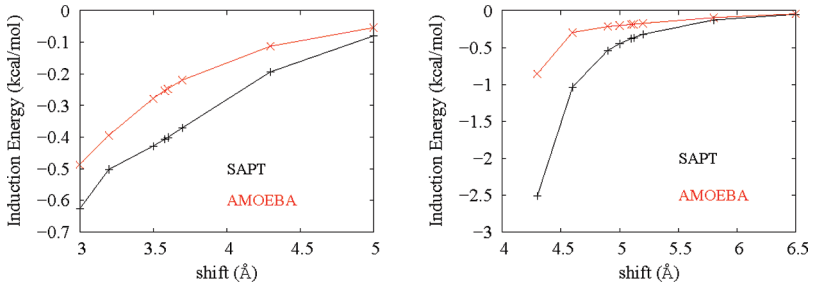

Figure 10. The induction energy for the graphite (left) and T-shaped (right) configuration of the naphthalene dimer (in kcal/mol). Shift is the distance (in Å) between the two naphthalene molecules. The reference data are taken from ref 57. Lines are drawn to guide the eye.

be judged from a direct comparison with the sum of induction and exchange−induction energies calculated using SAPT. However, this particular component is very difficult to obtain accurately in SAPT since third and higher order contributions might be significant as well (see, for example, refs 87−89). The reference data for the benzene dimer we used included third order contributions to the induction energy, and in Figure 9 we compare this data with the induction energy obtained with the standard AMOEBA parameters for a number of sandwich and T-shaped configurations. Overall, for nonpolar molecules, we expect the induction energy to be small in absolute terms compared to other contributions. We note that for the benzene dimer configurations shown in Figure 9, the AMOEBA overestimates (underestimates) the reference values of induction energy at smaller intermonomer separations for the sandwich (T-shaped) dimer configurations. For naphthalene, only second order contributions were included in the SAPT calculations.[57] As can be seen from Figure 10, the AMOEBA force field systematically underestimates the induction energy for some representative configurations, especially so for the T-shaped ones.

To check the reliability of the AMOEBA parameters, we can, in addition, compare the static molecular polarizability tensors (α) calculated at different levels of theory with those obtained from the AMOEBA force field by iterating the induced dipoles to self-consistency, as implemented in TINKER. Table 3 presents the results (see Figure 6 for the axes definition), where experimental data are also given for comparison. Due to the high symmetry of the molecules, only diagonal elements of the polarizability tensors are nonzero. An examination of Table 3 shows that the components of the static molecular polarizability tensor calculated in this work at the DFT level (B3LYP/aug-cc-pVDZ) match closely their counterparts obtained using the linear response coupled cluster approach (CCSD) by Hammond et al.[90] We also note that the calculated molecular polarizabilities (DFT/CCSD) are well reproduced by the force field, especially for the less polarizable perpendicular direction (Z axis). At the same time, it can be seen that for larger PAHs, the agreement is less perfect for the long molecular axis (X), where the polarizability is underestimated by the AMOEBA force field. Despite the fact that refining the atomic polarizability parameters would improve the agreement, it is our belief that some degree of anisotropy should be included in the model[91] to get more accurate results (compared to the "exact" values)[33] for the induction energy.

van der Waals Energy. As already mentioned above, we adopted the functional form for the vdW energy (repulsion−dispersion) used in the AMOEBA force field and reoptimized the two parameters for each atom class (atom size, r, and well depth, ε) based on the sum of the three separate contributions calculated using SAPT, namely, exchange−repulsion, dispersion, and exchange−dispersion. Table 4 compares the old and the new values for aromatic carbon and hydrogen atoms taken as an average from the refinements on the naphthalene and anthracene dimers.[57]

With the new vdW parameters, we can reproduce the SAPT reference data with RMS deviations (the mean difference in parentheses) of 0.5 (0.17), 0.5 (−0.18), and 0.9 (0.05) kcal/mol for naphthalene (35 configurations), anthracene (32 configurations), and pyrene (41 configurations) dimers, respectively. For pyrene, we excluded three dimer configurations with the shortest intermonomer distance (2.8 Å) from the reference data set. Figure 11 displays the scatter plots for these three PAH dimers. It can be seen from this figure that with the reoptimized vdW parameters from Table 4 ("new"), we can reproduce the reference data over a wide range of energy values. Even the

Table 3. Molecular Polarizability Tensors (in Å^3) for Benzene and Several PAHs

method	α_{xx}	α_{yy}	α_{zz}	α_{iso}[a]
		benzene		
DFT[b]	12.17	12.17	6.64	10.33
TDDFT[93]	12.26	12.26	6.61	10.38
CCSD[90]	11.89	11.89	6.60	10.13
CCSD[92]	12.06	12.06	6.37	10.16
AMOEBA[c]	12.24	12.24	6.64	10.37
exp[93]	12.20	12.20	7.28	10.56
		naphthalene		
DFT	25.58	18.60	9.80	17.99
TDDFT[94]	26	19	10	18
CCSD[90]	24.69	18.28	9.84	17.60
AMOEBA	21.89	18.50	9.77	16.72
exp[95]	24.39	18.20	9.60	17.40
		anthracene		
DFT	44.06	25.09	12.89	27.35
TDDFT[94]	46	26	13	28
CCSD[90]	41.73	24.60	12.98	26.44
AMOEBA	32.62	24.56	12.93	23.37
exp[96]	35.90	24.46	15.88	25.41
		pyrene		
DFT	44.17	31.87	13.92	29.98
TDDFT[94]	45	32	14	30
CCSD[90]	42.37	31.14	na	na
AMOEBA	33.70	29.81	13.75	25.75
exp[97]	34.2	34.2	16.3	28.2
		perylene		
DFT	55.97	44.01	16.82	38.94
TDDFT[94]	56	44	16	39
AMOEBA	42.90	38.16	16.95	32.67
exp[98]	57	46	16	40
		coronene		
DFT	59.12	59.12	18.96	45.73
TDDFT[94]	61	61	19	47
AMOEBA	47.51	47.51	19.14	38.05
exp[99]	56.8	56.8	20.7	44.8

[a] Isotropic polarizability taken as $1/3(\alpha_{xx} + \alpha_{yy} + \alpha_{zz})$. [b] At the B3LYP/aug-cc-pVDZ//B3LYP/6-31G(d) level. [c] Interactive molecular polarizability.

energies in a very "repulsive" region of the PAH dimers are accurately modeled. For both configurations of the benzene dimer, the agreement with the SAPT reference data is also improved compared to the other force fields (see Figures 2 and 3).

Total Intermolecular Energy. We calculate the total intermolecular interaction energy by summing up the electrostatic (both short- and long-range components), vdW, and induction contributions. We reproduce the total reference energies from SAPT with RMS deviations (the mean difference in parentheses) of 0.64 (−0.45), 0.9 (−0.7), and 0.5 (−0.13) kcal/mol for naphthalene, anthracene, and pyrene dimers, respectively. For PAHs, we recommend using values for the expansion−contraction parameters of 1.02 and 1.4 for carbon and hydrogen atoms, respectively, together with the new vdW parameters listed in Table 4. Examination of Figure 12 and of the mean differences shows that some systematic bias is present, especially for the naphthalene and anthracene dimers, which is probably due to inaccuracies in the induction term (underestimated by the force field) that warrant further investigation. By comparison, with the unmodified AMOEBA force field, the RMS deviations are 2.9 (naphthalene), 4.0 (anthracene), and 2.6 (pyrene) kcal/mol.

Table 4. van der Waals Parameters for Carbon and Hydrogen Atom Classes for the AMOEBA Force Field

	old		new	
atom class	r, Å	ε, kcal/mol	r, Å	ε, kcal/mol
C	3.800	0.089	4.285	0.050
H	2.980	0.026	2.560	0.0075

To further validate our new force field, we performed a full crystal energy minimization by optimizing over fractional atomic coordinates and the lattice parameters for benzene, naphthalene, anthracene, pyrene, and coronene. To make the comparison with the experimental crystal structures meaningful, the internal flexibilities of the molecules are taken into account using the standard AMOEBA parameters (atom classes 85 and 86 for the aromatic carbon and hydrogen atoms from the amoeba09.prm compilation, respectively). Table 5 presents the results.

Examination of this table shows that the AMOEBA force field poorly reproduces the orthorhombic lattice of the benzene crystal (space group *Pbca*), whereas the unit cell edges based on our new force field (labeled as "new" in Table 5) closely match the experimental data. Ab initio calculations of van der Waals bonded molecular crystals, such as solid benzene, are notoriously difficult to perform accurately. That this is still a challenge is evident from the comparison of the lattice parameters fully optimized by Bucko et al. (ref 100 and references therein) with the VASP program. A closer examination of the unit cell of the solid benzene, in which the four molecules are arranged in an edge-to-face manner at 87° angles pairwise,[101] reveals the dominant contribution of this type of tilted T-shaped configuration, shown in Figure 1. We note that this particular configuration is found to be one of the most stable in the gas phase benzene dimer (see, for example, ref 48), and it persists in the solid benzene even under high pressure.[110] As is evident from Figure 3 above, the total intermolecular interaction energies for this configuration at a center-of-mass distance of around 5.0 Å, as found in the crystal, are poorly reproduced by the AMOEBA force field as compared to the reference (SAPT) data. Our new force field, on the other hand, nicely reproduces the experimentally observed mutual arrangement of the four molecules in the unit cell, which is not the case with the AMOEBA force field. To investigate the importance of this short-range electrostatic contribution in more detail, we tested two other models, where (1) we reoptimized the four vdW parameters (two for both carbon and hydrogen) of the AMOEBA force field based on the total interaction energies for 500 configurations of the benzene dimer used before without adding the short-range electrostatic contribution and where (2) we included the short-range term without reoptimizing the vdW parameters. Despite the relatively small RMS deviation of ca. 1 kcal/mol for the whole set of benzene dimers, the model (1) was not capable of reproducing either the cell edges or the mutual arrangement of the four

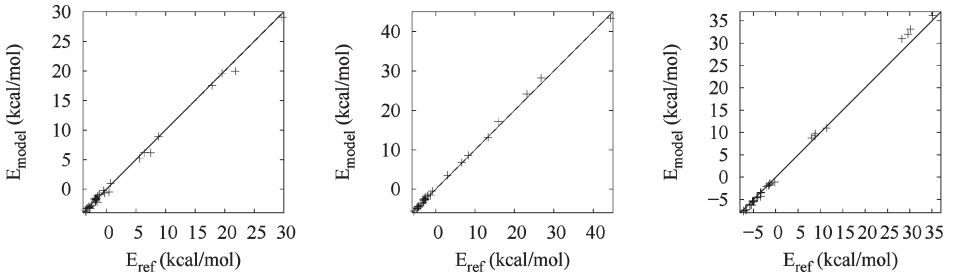

Figure 11. Scatter plots of van der Waals energies for selected dimers of PAHs (in kcal/mol). From left to right: naphthalene (35 configurations), anthracene (32 configurations), and pyrene (41 configurations). The reference data are taken from Podeszwa et al.[57]

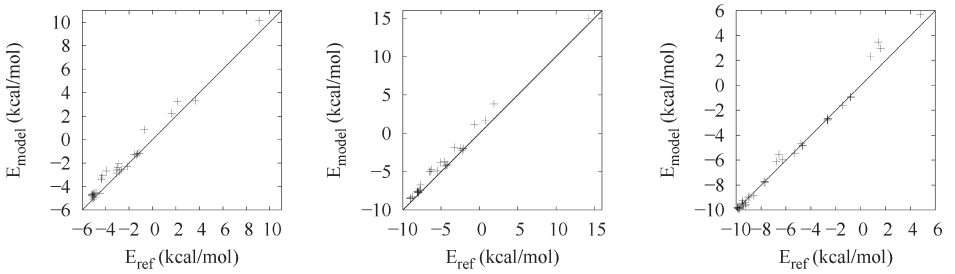

Figure 12. Scatter plots of total intermolecular energies for selected dimers of PAHs (in kcal/mol). From left to right: naphthalene (35 configurations), anthracene (32 configurations), and pyrene (41 configurations). The reference data are taken from Podeszwa et al.[57]

benzene molecules in the unit cell, the results being close to those obtained with the standard AMOEBA force field. Our second model, on the other hand, was found to be in much better agreement with our new force field model, qualitatively reproducing the mutual arrangement of the benzene molecules observed in the experimental crystal structure. This indicates that the short-range electrostatic contribution seems to be particularly important for the intermolecular interaction for a T-shaped configuration in π-conjugated systems (for a discussion, see also refs 111 and 112). It would be interesting to see whether our new force field is able to reproduce (or even predict) high-pressure polymorphs of the solid benzene.[113] For PAHs, the situation is different in a sense that the $\pi-\pi$ stacking interactions are now competitive with those found in (more electrostatically controlled) T-shaped configurations.[112] From Table 5, it can be seen that the experimental monoclinic lattices (space group $P2_1/a$) of selected PAHs are reproduced by the force fields. Recently, Sanchez-Carrera et al.[103] optimized the unit cell parameters for a number of oligocenes from naphthalene to pentacene using a different program (DMAREL) and a different force field (Buckingham exp-6 for vdW interactions along with ESP-fitted point charges for electrostatics) within the framework of the rigid-molecule approximation (experimental molecular geometries were used). Despite the markedly different approaches used, their results are in agreement both with ours and with the experiment. Interestingly, our new force field somewhat overestimates the length of the *a* axis of the unit cell for naphthalene and anthracene. At the same time, the lengths of the other two lattice axes (*b* and *c*) for naphthalene are closer to the experimental data than those obtained with the standard AMOEBA force field. It should be also noted that for pyrene the standard AMOEBA force field gave the optimized lattice parameters observed for the low-temperature (T = 93 K) metastable phase (II), regardless of the starting values, whereas our new force field recovers the parameters for both solid phases. It is well-known that lattice energies are important for assessing the quality of a force field. Our values for naphthalene (−12.0 kcal/mol) and anthracene (−16.6 kcal/mol) underestimated the experimental values[114] of −17.8 (naphthalene) and −23.9 (anthracene) kcal/mol mainly due to somewhat larger *a* axis of the unit cell.

Overall, in contrast to the standard AMOEBA and other empirical force fields,[103] our proposed intermolecular force field parameters are based solely on the properties of monomers calculated from first principles. Indeed, the atomic multipoles come from the distributed multipole analysis (GDMA) based on the monomer wave function, whereas the short-range electrostatic contribution and the vdW parameters were fitted to reproduce the corresponding terms of the SAPT interaction energy, the latter being calculated directly as a sum of physically meaningful contributions. The reason we use the data calculated by SAPT as a reference is that in this type of rigorous perturbation theory the physically meaningful components (first-order electrostatic and exchange contributions and second-order induction and dispersion terms) can be nicely correlated with the terms usually included in current empirical force fields. This would be, however, not so straightforward with some other decomposition schemes, such as the ones described in Khaliullin et al.[115] or in Wu et al.,[116] where the electrostatic and exchange contributions are not separated (named as the frozen density component there). It would be interesting to try to parametrize a force field using this latter (variational) decomposition scheme as well. It is also worth remarking that the quality of our new force field cannot be better than the quality of the reference data it is based upon, so that our parameters will definitely benefit from further improvement of the reference data. Furthermore, we are confident that the notoriously difficult task of crystal structure prediction can benefit from the force field development strategy presented in this work.[117] We also hope that our contribution can help better understand the shortcomings and failures of the currently used force fields and will ultimately lead to an

Table 5. Unit Cell Parameters for Benzene and Selected PAHs

	a (Å)	b (Å)	c (Å)	α (deg)	β (deg)	γ (deg)
			benzene			
AMOEBA	7.744	7.750	7.750	90.0	90.0	90.0
new	7.567	9.269	7.142	90.0	90.0	90.0
VASP[101]	7.09	9.07	6.54	90.0	90.0	90.0
exp (138 K)[102]	7.39	9.42	6.81	90.0	90.0	90.0
exp (4.2 K)[102]	7.3551	9.3712	6.6994	90.0	90.0	90.0
			naphthalene			
AMOEBA	8.206	5.512	9.143	90.0	125.2	90.0
new	8.539	5.884	8.954	90.0	122.6	90.0
DMAREL[103]	8.146	6.033	8.716	90.0	122.5	90.0
exp[104]	8.108	5.940	8.647	90.0	124.4	90.0
			anthracene			
AMOEBA	8.361	6.080	11.070	90.0	127.0	90.0
new	8.896	6.121	11.184	90.0	124.6	90.0
DMAREL[103]	8.361	6.116	11.167	90.0	123.5	90.0
exp[105]	8.414	5.990	11.095	90.0	125.3	90.0
			pyrene (I)			
AMOEBA	12.513	9.799	8.104	90.0	94.7	90.0
new	13.637	9.435	8.528	90.0	100.2	90.0
exp[106]	13.532	9.159	8.387	90.0	100.2	90.0
			pyrene (II)			
AMOEBA	12.510	9.800	8.105	90.0	94.7	90.0
new	12.635	10.177	8.468	90.0	98.1	90.0
exp[107,108]	12.358	10.020	8.260	90.0	96.5	90.0
			coronene			
AMOEBA	16.156	4.484	9.934	90.0	110.2	90.0
new	16.186	5.047	9.904	90.0	110.8	90.0
exp[109]	16.119	4.702	10.102	90.0	110.9	90.0

improvement in the quality of future force fields for molecular simulations. Curiously, in a very recent study on the development of polarizable models for calculating interactions between atomic charges and induced point dipoles, Wang et al.[118] pointed out the difficulty in reproducing interaction energies (at the MP2/aug-cc-pVTZ level) for molecules possessing aromatic groups (even after reoptimization of the van der Waals parameters). They found out that all MM models investigated (including nonpolarizable or fixed-charge ones) have a tendency to underestimate the attractive force between the aromatic moieties. Even if it is known that the MP2 method (corrected for basis set superposition error) overestimates the binding energy for π stacks (see, for example, ref 119), we believe that a further improvement can be achieved by including more physically grounded electrostatics in a force field, which is the main topic of our work. There is a hint in a recent work of Watanabe et al.[120] that an accurate treatment of electrostatic interactions between adsorbates and a host framework would necessitate the inclusion of charge penetration effects as well.

One final note is appropriate at this point. Since accurate reference data based on the intermolecular perturbation theory (such as SAPT) are still relatively scarce, a viable strategy using the total intermolecular energy from highly accurate supermolecule calculations can be used for the parametrization (see, for example, refs 121−123). In this case, first, the short-range electrostatic contribution can be parametrized using a much cheaper method (e.g., B3LYP/aug-cc-pVXZ, X = D or T), as is done here for the perylene dimer, and, second, when an appropriate model for the induction (polarization) contribution is at hand, the vdW parameters for a chosen functional form can be optimized to reproduce the repulsion−dispersion contribution taken as the difference between the total interaction energy (as reference) and the sum of the electrostatic (including both the short- and long-range terms) and induction contributions. As an example, we took the data published recently by Sherrill and co-workers[49] for the benzene dimer (∼90 configurations including sandwich, T-shaped, and parallel-displaced ones) calculated with the coupled-cluster theory through perturbative triples, CCSD(T), extrapolated to the complete basis set limit. Having parametrized the short-range part of the electrostatic energy (see Table 1 for expansion−contraction parameters) and utilizing the induced point dipoles method (AMOEBA) to treat polarization, the reoptimized vdW parameters (r = 4.239 Å and ε = 0.0726 kcal/mol for carbon and r = 2.553 Å and ε = 0.0043 kcal/mol for hydrogen) turned out to be similar to the values (labeled "new") shown in Table 4. With these force field parameters at hand, we can reproduce perfectly both the lattice parameters of the orthorhombic phase of solid benzene (a = 7.391 Å, b = 9.356 Å, and c = 6.891 Å) and the mutual arrangement of the four molecules in the unit cell as before using the SAPT data as a reference. In addition, the calculated lattice energy of −10.2 kcal/mol (at T = 0 K and without zero-point energy correction), which is known to be notoriously difficult to evaluate reliably, is in very good agreement with the values estimated from first-principles methods[124−126,100] (see also refs 127−129) and the experimental value (−11.3 kcal/mol).[114]

5. CONCLUSIONS

Motivated by the need for a force field that can capture the right physics of intermolecular interactions, we incorporated an extra pairwise-additive energy term, which describes the short-range contribution to the electrostatic energy due to charge penetration, into the AMOEBA polarizable force field.[46] Following the original ideas of Spackman,[50] the expansion−contraction parameters are proposed to modify the radial dependence of the spherical atomic charge densities. For a series of PAHs, we were able to show that with a limited number of these parameters, the intermolecular electrostatic energies estimated by the force field match nicely the reference data based on SAPT interaction energy calculations. Taken together with the reoptimized van der Waals contribution, a balanced force field can be readily constructed which avoids to a large extent the error cancellation between different terms in the force field. Having implemented the gradients of this new term, we are now in a position to perform static geometry optimizations as well as molecular dynamics simulations on the aggregation of PAH clusters, the outcome of which being relevant for a number of fields such as soot formation in combustion,[130] interstellar radiation,[131] optoelectronic devices,[6] supramolecular chemistry (as exemplified by molecular tweezers[132]), and host−guest systems,[133] to name a few. Moreover, we can anticipate that incorporating realistic electrostatic effects into a force field would allow the development of much more accurate QM/MM embedding schemes. Polycyclic aromatic hydrocarbons and their derivatives

are seen as a promising class of materials for optoelectronics and organic solar cells. Understanding the charge and energy transport through these materials is very important in tuning their properties for a particular application. We hope that physically realistic force fields would be indispensable for that purpose, and work along these lines is in progress.

AUTHOR INFORMATION

Corresponding Author

*E-mail: bernd.engels@mail.uni-wuerzburg.de; maxim.tafipolski@uni-wuerzburg.de.

ACKNOWLEDGMENT

We are grateful to the Deutsche Forschungsgemeinschaft (GRK1221, SFB 630) and the Volkswagen Stiftung for financial support. M.T. would like to thank Professor Rafał Podeszwa, Professor Krzysztof Szalewicz, and Dr. Konrad Patkowski for very fruitful discussions and data provided relating to work reported in ref 57 and Dr. Anatoliy Volkov for providing the SPDF program and many useful suggestions.

REFERENCES

(1) Engkvist, O.; Astrand, P. O.; Karlstrom, G. *Chem. Rev.* **2000**, *100*, 4087.
(2) Chipot, C.; Angyan, J. G. *New J. Chem.* **2005**, *29*, 411.
(3) Stone, A. J. *Science* **2008**, *321*, 787.
(4) Janowski, T.; Ford, A. R.; Pulay, P. *Mol. Phys.* **2010**, *108*, 249.
(5) Sherrill, C. D. In *Rev. Comput. Chem.*; Lipkowitz, K. B., Cundari, T. R., Eds.; Wiley: New York, 2009; Vol. 26, Chapter 1, pp 1−38.
(6) Bredas, J. L.; Beljonne, D.; Coropceanu, V.; Cornil, J. *Chem. Rev.* **2004**, *104*, 4971.
(7) Stone, A. J. *The Theory of Intermolecular Forces*; Oxford University Press: Oxford, U.K., 1996.
(8) Kaplan, I. G. *Intermolecular Interactions*; John Wiley & Sons, Inc.: New York, 2006.
(9) Chen, W.; Gordon, M. S. *J. Phys. Chem.* **1996**, *100*, 14316.
(10) Piquemal, J.-P.; Chevreau, H.; Gresh, N. *J. Chem. Theory Comput.* **2007**, *3*, 824.
(11) Stone, A. J.; Misquitta, A. J. *Int. Rev. Phys. Chem.* **2007**, *26*, 193.
(12) Podeszwa, R.; Bukowski, R.; Szalewicz, K. *J. Phys. Chem. A* **2006**, *110*, 10345.
(13) Tekin, A.; Jansen, G. *Phys. Chem. Chem. Phys.* **2007**, *9*, 1680.
(14) Fiethen, A.; Jansen, G.; Hesselmann, A.; Schuetz, M. *J. Am. Chem. Soc.* **2008**, *130*, 1802.
(15) Pitonak, M.; Riley, K. E.; Neogrady, P.; Hobza, P. *ChemPhysChem* **2008**, *9*, 1636.
(16) Cybulski, H.; Sadlej, J. *J. Chem. Theory Comput.* **2008**, *4*, 892.
(17) Geng, Y.; Takatani, T.; Hohenstein, E. G.; Sherrill, C. D. *J. Phys. Chem. A* **2010**, *114*, 3576.
(18) Hohenstein, E. G.; Sherrill, C. D. *J. Chem. Phys.* **2010**, *133*, 014101.
(19) Hesselmann, A.; Korona, T. *Phys. Chem. Chem. Phys.* **2011**, *13*, 732.
(20) Riley, K. E.; Pitonak, M.; Jurecka, P.; Hobza, P. *Chem. Rev.* **2010**, *110*, 5023.
(21) Hohenstein, E. G.; Sherrill, C. D. *J. Chem. Phys.* **2010**, *132*, 184111.
(22) Misquitta, A. J.; Szalewicz, K. *J. Chem. Phys.* **2005**, *122*, 214109.
(23) Hesselmann, A.; Jansen, G.; Schutz, M. *J. Chem. Phys.* **2005**, *122*, 014103.
(24) Jeziorski, B.; Moszynski, R.; Szalewicz, K. *Chem. Rev.* **1994**, *94*, 1887.
(25) Mooij, W. T. M.; van Duijneveldt, F. B.; van Duijneveldt-van de Rijdt, J. G. C. M.; van Eijck, B. P. *J. Phys. Chem. A* **1999**, *103*, 9872.
(26) Mitchell, J. B. O.; Price, S. L. *J. Phys. Chem. A* **2000**, *104*, 10958.
(27) Hloucha, M.; Sum, A. K.; Sandler, S. I. *J. Chem. Phys.* **2000**, *113*, 5401.
(28) Torheyden, M.; Jansen, G. *Mol. Phys.* **2006**, *104*, 2101.
(29) Li, X.; Volkov, A. V.; Szalewicz, K.; Coppens, P. *Acta Crystallogr., Sect. D* **2006**, *62*, 639.
(30) Szalewicz, K.; Leforestier, C.; van der Avoird, A. *Chem. Phys. Lett.* **2009**, *482*, 1.
(31) Archambault, F.; Chipot, C.; Soteras, I.; Javier Luque, F.; Schulten, K.; Dehez, F. *J. Chem. Theory Comput.* **2009**, *5*, 3022.
(32) Wang, B.; Truhlar, D. G. *J. Chem. Theory Comput.* **2010**, *6*, 3330.
(33) Totton, T. S.; Misquitta, A. J.; Kraft, M. *J. Chem. Theory Comput.* **2010**, *6*, 683.
(34) Sherrill, C. D.; Sumpter, B. G.; Sinnokrot, M. O.; Marshall, M. S.; Hohenstein, E. G.; Walker, R. C.; Gould, I. R. *J. Comput. Chem.* **2009**, *30*, 2187.
(35) Paton, R. S.; Goodman, J. M. *J. Chem. Inf. Model.* **2009**, *49*, 944.
(36) Morgado, C. A.; Jurecka, P.; Svozil, D.; Hobza, P.; Sponer, J. *J. Chem. Theory Comput.* **2009**, *5*, 1524.
(37) Morgado, C. A.; Jurecka, P.; Svozil, D.; Hobza, P.; Sponer, J. *Phys. Chem. Chem. Phys.* **2010**, *12*, 3522.
(38) Zgarbova, M.; Otyepka, M.; Sponer, J.; Hobza, P.; P., J. *Phys. Chem. Chem. Phys.* **2010**, *12*, 10476.
(39) Kolar, M.; Berka, K.; Jurecka, P.; Hobza, P. *ChemPhysChem* **2010**, *11*, 2399.
(40) Nemkevich, A.; Buergi, H.-B.; Spackman, M. A.; Corry, B. *Phys. Chem. Chem. Phys.* **2010**, *12*, 14916.
(41) Rutledge, L. R.; Wetmore, S. D. *Can. J. Chem.* **2010**, *88*, 815.
(42) Tateno, M.; Hagiwara, Y. *J. Phys.: Condens. Matter* **2009**, *21*, 064243.
(43) Jorgensen, W. L.; Tirado-Rives, J. *J. Am. Chem. Soc.* **1988**, *110*, 1657.
(44) Allinger, N. L.; Yuh, Y. H.; Lii, J.-H. *J. Am. Chem. Soc.* **1989**, *111*, 8551.
(45) Allinger, N. L.; Li, F. B.; Yan, L. Q.; Tai, J. C. *J. Comput. Chem.* **1990**, *11*, 868.
(46) Ponder, J. W.; Wu, C.-J.; Ren, P.-Y.; Pande, V. S.; Chodera, J. D.; Schnieders, M. J.; Haque, I.; Mobley, D. L.; Lambrecht, D. S.; DiStasio, R. A., Jr.; Head-Gordon, M.; Clark, G. N. I.; Johnson, M. E.; Head-Gordon, T. *J. Phys. Chem. B* **2010**, *114*, 2549.
(47) Tinker software tools for molecular design: Ponder, J. W.; Ren, P.; Pappu, R. V.; Hart, R. K.; Hodgson, M. E.; Cistola, D. P.; Kundrot, C. E.; Richards, F. M. *Tinker*, version 5.1; Washington University School of Medicine: St. Louis, MO, 2010. http://dasher.wustl.edu/tinker/ (accessed 02/27/2011).
(48) van der Avoird, A.; Podeszwa, R.; Szalewicz, K.; Leforestier, C.; van Harrevelt, R.; Bunker, P. R.; Schnell, M.; von Helden, G.; Meijer, G. *Phys. Chem. Chem. Phys.* **2010**, *12*, 8219.
(49) Sherrill, C. D.; Takatani, T.; Hohenstein, E. G. *J. Phys. Chem. A* **2009**, *113*, 10146.
(50) Spackman, M. A. *Chem. Phys. Lett.* **2006**, *418*, 158.
(51) Slipchenko, L. V.; Gordon, M. S. *Mol. Phys.* **2009**, *107*, 999.
(52) Cisneros, G. A.; Tholander, S. N.-I.; Parisel, O.; Darden, T. A.; Elking, D.; Perera, L.; Piquemal, J. P. *Int. J. Quantum Chem.* **2008**, *108*, 1905.
(53) Wheatley, R. J. *Mol. Phys.* **1993**, *79*, 597.
(54) Elking, D. M.; Cisneros, G. A.; Piquemal, J.-P.; Darden, T. A.; Pedersen, L. G. *J. Chem. Theory Comput.* **2010**, *6*, 190.
(55) Stone, A. J.; Price, S. L. *J. Phys. Chem.* **1988**, *92*, 3325.
(56) Freitag, M. A.; Gordon, M. S.; Jensen, J. H.; Stevens, W. J. *J. Chem. Phys.* **2000**, *112*, 7300.
(57) Podeszwa, R.; Szalewicz, K. *Phys. Chem. Chem. Phys.* **2008**, *10*, 2735.
(58) Podeszwa, R. *J. Chem. Phys.* **2010**, *132*, 044704.
(59) Price, S. L.; Leslie, M.; Welch, G. W. A.; Habgood, M.; Price, L. S.; Karamertzanis, P. G.; Day, G. M. *Phys. Chem. Chem. Phys.* **2010**, *12*, 8478.

(60) Shaik, M. S.; Devereux, M.; Popelier, P. L. A. *Mol. Phys.* **2008**, *106*, 1495.
(61) Stone, A. J.; Alderton, M. *Mol. Phys.* **1985**, *56*, 1047.
(62) Stone, A. J. *J. Chem. Theory Comput.* **2005**, *1*, 1128. GDMA 2.2.04 at http://www−stone.ch.cam.ac.uk/programs.html (accessed 02/27/2011).
(63) Frisch, M. J.; Trucks, G. W.; Schlegel, H. B.; Scuseria, G. E.; Robb, M. A.; Cheeseman, J. R.; Montgomery, J. A., Jr.; Vreven, T.; Kudin, K. N.; Burant, J. C.; Millam, J. M.; Iyengar, S. S.; Tomasi, J.; Barone, V.; Mennucci, B.; Cossi, M.; Scalmani, G.; Rega, N.; Petersson, G. A.; Nakatsuji, H.; Hada, M.; Ehara, M.; Toyota, K.; Fukuda, R.; Hasegawa, J.; Ishida, M.; Nakajima, T.; Honda, Y.; Kitao, O.; Nakai, H.; Klene, M.; Li, X.; Knox, J. E.; Hratchian, H. P.; Cross, J. B.; Adamo, C.; Jaramillo, J.; Gomperts, R.; Stratmann, R. E.; Yazyev, O.; Austin, A. J.; Cammi, R.; Pomelli, C.; Ochterski, J. W.; Ayala, P. Y.; Morokuma, K.; Voth, G. A.; Salvador, P.; Dannenberg, J. J.; Zakrzewski, V. G.; Dapprich, S.; Daniels, A. D.; Strain, M. C.; Farkas, O.; Malick, D. K.; Rabuck, A. D.; Raghavachari, K.; Foresman, J. B.; Ortiz, J. V.; Cui, Q.; Baboul, A. G.; Clifford, S.; Cioslowski, J.; Stefanov, B. B.; Liu, G.; Liashenko, A.; Piskorz, P.; Komaromi, I.; Martin, R. L.; Fox, D. J.; Keith, T.; Al-Laham, M. A.; Peng, C. Y.; Nanayakkara, A.; Challacombe, M.; Gill, P. M. W.; Johnson, B.; Chen, W.; Wong, M. W.; Gonzalez, C.; Pople, J. A. *Gaussian 03*, Revision C.02; Gaussian, Inc.: Wallingford, CT, 2004.
(64) Becke, A. D. *Phys. Rev. A* **1988**, *38*, 3098.
(65) Becke, A. D. *J. Chem. Phys.* **1993**, *98*, 5648.
(66) Lee, C.; Yang, W.; Parr, R. G. *Phys. Rev. B* **1988**, *37*, 785.
(67) Dunning, T. H. *J. Chem. Phys.* **1989**, *90*, 1007.
(68) Volkov, A.; Coppens, P. *J. Comput. Chem.* **2004**, *25*, 921.
(69) Kisiel, Z. *MIN16*; Institute of Physics, Polish Academy of Sciences: Warszawa, Poland. http://info.ifpan.edu.pl/~kisiel/model/model.htm (accessed 02/27/2011).
(70) Clementi, E.; Roetti, C. *At. Data Nucl. Data Tables* **1974**, *14*, 177.
(71) Bunge, C. F.; Barrientos, J. A.; Bunge, A. V. *At. Data Nucl. Data Tables* **1993**, *53*, 113.
(72) Su, Z. W.; Coppens, P. *Acta Crystallogr., Sect. A* **1998**, *54*, 646. Available at http://harker.chem.buffalo.edu/group/wavtable.html (accessed 02/27/2011).
(73) Su, Z.; Coppens, P. *J. Appl. Crystallogr.* **1990**, *23*, 71.
(74) Destro, R.; Soave, R.; Barzaghi, M. *J. Phys. Chem. B* **2008**, *112*, 5163.
(75) Coppens, P.; Guru Row, T. N.; Leung, P.; Stevens, E. D.; Becker, P. J.; Yang, Y. W. *Acta Crystallogr., Sect. A* **1979**, *35*, 63.
(76) Press, W. H.; Teukolsky, S.; Vetterling, W.; Flannery, B. *Numerical Recipes in Fortran 77. The Art of Scientific Computing*, 2nd ed.; Cambridge University Press: Cambridge, U. K., 1992; p 136.
(77) Halgren, T. A. *J. Am. Chem. Soc.* **1992**, *114*, 7827.
(78) Mkadmh, A. M.; Hinchliffe, A.; Abu-Awwad, F. M. *THEOCHEM* **2009**, *901*, 9.
(79) Charbonneau, P. *Astrophys. J. Suppl. S* **1995**, *101*, 309. PIKAIA 1.2 at http://www.hao.ucar.edu/modeling/pikaia/pikaia.php (accessed 02/27/2011).
(80) Tafipolsky, M.; Schmid, R. *J. Phys. Chem. B* **2009**, *113*, 1341.
(81) Volkov, A.; King, H.; Coppens, P. *J. Chem. Theory Comput.* **2006**, *2*, 81.
(82) Obolensky, O. I.; Semenikhina, V. V.; Solov'yov, A. V.; Greiner, W. *Int. J. Quantum Chem.* **2007**, *107*, 1335.
(83) Malloci, G.; Joblin, C.; Mulas, G. *Chem. Phys.* **2007**, *332*, 353. See also http://astrochemistry.ca.astro.it/database/pahs.html (accessed 02/27/2011).
(84) Besler, B. H.; Merz, K. M.; Kollman, P. A. *J. Comput. Chem.* **1990**, *11*, 431.
(85) Camerman, A.; Trotter, J. *Proc. R. Soc. London, Ser. A* **1964**, *279*, 129.
(86) Jenness, G. R.; Karalti, O.; Jordan, K. D. *Phys. Chem. Chem. Phys.* **2010**, *12*, 6375.
(87) Misquitta, A. J.; Stone, A. J. *J. Chem. Theory Comput.* **2008**, *4*, 7.
(88) Misquitta, A. J.; Stone, A. J.; Price, S. L. *J. Chem. Theory Comput.* **2008**, *4*, 19.
(89) Patkowski, K.; Szalewicz, K.; Jeziorski, B. *Theor. Chem. Acc.* **2010**, *127*, 211.
(90) Hammond, J. R.; Kowalski, K.; deJong, W. A. *J. Chem. Phys.* **2007**, *127*, 144105.
(91) Mayer, A.; Astrand, P.-O. *J. Phys. Chem. A* **2008**, *112*, 1277.
(92) Jiemchooroj, A.; Norman, P.; Sernelius, B. E. *J. Chem. Phys.* **2005**, *123*, 124312.
(93) Ritchie, G. L. D.; Watson, J. N. *Chem. Phys. Lett.* **2000**, *322*, 143.
(94) Marques, M. A. L.; Castro, A.; Malloci, G.; Mulas, G.; Botti, S. *J. Chem. Phys.* **2007**, *127*, 014107.
(95) Vuks, M. F. *Opt. Spectrosc.* **1966**, *20*, 361.
(96) LeFevre, R. J. W.; Radom, L.; Ritchie, G. L. D. *J. Chem. Soc. B* **1968**, 775.
(97) Cheng, C. L.; Murthy, D. S. N.; Ritchie, G. L. D. *Aust. J. Chem.* **1972**, *25*, 1301.
(98) Liptay, W. *Z. Naturforsch.* **1972**, *A 27*, 1336.
(99) LeFevre, R. J. W.; Sundaram, K. M. *J. Chem. Soc.* **1963**, 4442.
(100) Bucko, T.; Hafner, J.; Lebegue, S.; Angyan, J. G. *J. Phys. Chem. A* **2010**, *114*, 11814.
(101) Bacon, G. E.; Curry, N. A.; Wilson, S. A. *Proc. R. Soc. London, Ser. A* **1964**, *279*, 98.
(102) David, W. I. F.; Ibberson, R. M.; Jeffrey, G. A.; Ruble, J. R. *Physica B* **1992**, *180*, 597.
(103) Sanchez-Carrera, R. S.; Paramonov, P.; Day, G. M.; Coropceanu, V.; Bredas, J.-L. *J. Am. Chem. Soc.* **2010**, *132*, 14437.
(104) Brock, C. P.; Dunitz, J. D. *Acta Crystallogr., Sect. B* **1982**, *38*, 2218.
(105) Brock, C. P.; Dunitz, J. D. *Acta Crystallogr., Sect. B* **1990**, *46*, 795.
(106) Kai, Y.; Hama, F.; Yasuoka, N.; Kasai, N. *Acta Crystallogr., Sect. B* **1978**, *34*, 1263.
(107) Frampton, C. S.; Knight, K. S.; Shankland, N.; Shankland, K. *J. Mol. Struct.* **2000**, *520*, 29.
(108) Allen, F. H. *Acta Crystallogr., Sect. B* **2002**, *58*, 380.
(109) Fawcett, J. K.; Trotter, J. *Proc. R. Soc. London, Ser. A* **1966**, *289*, 366.
(110) Budzianowski, A.; Katrusiak, A. *Acta Crystallogr., Sect. B* **2006**, *62*, 94.
(111) Price, S. L.; Stone, A. J. *J. Chem. Phys.* **1987**, *86*, 2859.
(112) Williams, D. E.; Xiao, Y. L. *Acta Crystallogr., Sect. A* **1993**, *49*, 1.
(113) Raiteri, P.; Martonak, R.; Parrinello, M. *Angew. Chem., Int. Ed.* **2005**, *44*, 3769.
(114) Chickos, J. S.; Acree, W. E. *J. Phys. Chem. Ref. Data* **2002**, *31*, 537–698.
(115) Khaliullin, R. Z.; Cobar, E. A.; Lochan, R. C.; Bell, A. T.; Head-Gordon, M. *J. Phys. Chem. A* **2007**, *111*, 8753.
(116) Wu, Q.; Ayers, P. W.; Zhang, Y. K. *J. Chem. Phys.* **2009**, *131*, 164112.
(117) Day, G. M. *Crystallogr. Rev.* **2011**, *17*, 3.
(118) Wang, J. M.; Cieplak, P.; Li, J.; Wang, J.; Cai, Q.; Hsieh, M. J.; Lei, H.; Luo, R.; Duan, Y. *J. Phys. Chem. B* **2011**, *115*, 3100.
(119) Hobza, P.; Selzle, H. L.; Schlag, E. W. *J. Phys. Chem.* **1996**, *100*, 18790.
(120) Watanabe, T.; Manz, T. A.; Sholl, D. S. *J. Phys. Chem. C* **2011**, *115*, 4824.
(121) Rezac, J.; Jurecka, P.; Riley, K. E.; Cerny, J.; Valdes, H.; Pluhackova, K.; Berka, K.; Rezac, T.; Pitonak, M.; Vondrasek, J.; Hobza, P. *Collect. Czech. Chem. Commun.* **2008**, *73*, 1261.
(122) Podeszwa, R.; Patkowski, K.; Szalewicz, K. *Phys. Chem. Chem. Phys.* **2010**, *12*, 5974.
(123) Takatani, T.; Hohenstein, E. G.; Malagoli, M.; Marshall, M. S.; Sherrill, C. D. *J. Chem. Phys.* **2010**, *132*, 144104.
(124) Ringer, A. L.; Sherrill, C. D. *Chem.—Eur. J.* **2008**, *14*, 2542.
(125) Podeszwa, R.; Rice, B. M.; Szalewicz, K. *Phys. Rev. Lett.* **2008**, *101*, 115503.
(126) Li, Y.; Lu, D.; Nguyen, H.-V.; Galli, G. *J. Phys. Chem. A* **2010**, *114*, 1944.
(127) Bludsky, O.; Rubes, M.; Soldan, P. *Phys. Rev. B* **2008**, *77*, 092103.

(128) Liu, Y.; Goddard, W. A., III. *J. Phys. Chem. Lett.* **2010**, *1*, 2550.
(129) Beran, G. J. O.; Nanda, K. *J. Phys. Chem. Lett.* **2010**, *1*, 3480.
(130) Sabbah, H.; Biennier, L.; Klippenstein, S. J.; Sims, I. R.; Rowe, B. R. *J. Phys. Chem. Lett.* **2010**, *1*, 2962.
(131) Tielens, A. G. G. M. *Annu. Rev. Astron. Astrophys.* **2008**, *46*, 289.
(132) Petitjean, A.; Khoury, R. G.; Kyritsakas, N.; Lehn, J. M. *J. Am. Chem. Soc.* **2004**, *126*, 6637.
(133) Greathouse, J. A.; Ockwig, N. W.; Criscenti, L. J.; Guilinger, T. R.; Pohl, P.; Allendorf, M. D. *Phys. Chem. Chem. Phys.* **2010**, *12*, 12621.